GLOBAL Gas Turbine NEWS

Volume 53, No. 7 • September 2014

In this issue

go.asme.org/IGTI
Email: igti@asme.org

Welcome to the September 2014 edition of the Global Gas Turbine News. This edition will provide a comprehensive review of ASME Turbo Expo 2014, as well as glimpse into the launch of the 2015 show in Montreal.

ASME Turbo Expo is officially entering into its 60th year of operation as the premier turbomachinery conference in the world. In this issue, the familiar Turbo Expo prestige, knowledge and community will be on display as another successful conference is completed. Reflection on the past, pondering of the present, and eager anticipation of the future is the current theme within the community. Germany was the ideal location for TE14 as the Gas Turbine celebrated its 75th anniversary in its home country. It was a great occasion for the gas turbine industry to reflect on its humble beginnings 75 years ago.

ASME Turbo Expo 2014 in Düsseldorf, Germany

Technology Reduces Life Cycle Cost

Situated at the border of the Rhine River, Düsseldorf is the capital of the highest populated German state, North-Rhine Westphalia. The Düsseldorf area contributes significantly to the German landscape of turbo-engine builders, which has been shaped by organizations like Siemens, Alstom, MAN Turbo & Diesel, ABB and Atlas Copco for energy generation and process engineering. In the aerospace sector, the best known companies are MTU and Rolls-Royce Germany. Lufthansa Technik and N3, a joint venture of the former with Rolls-Royce, provide repair and overhaul services. All of the previous and many smaller companies benefit from a rich network of world leading, specialized technical universities and research institutions. This vibrant environment was the perfect backdrop for the turbomachinery industry, which is equally engaged in pushing the limits and challenging existing solutions to create better, even more efficient turbo engines.

...Continued on next page

ASME TURBO EXPO 2014 Opening Session

The conference began with three leading figures in the industry addressing the 2014 conference theme, "Technology Reduces Life Cycle Cost." Pratyush Nag of Siemens, Dr. Karsten Mühlenfeld of Rolls-Royce Deutschland, and Charles Soothill of Alstom Switzerland, examined the changes that are occurring in the industry and discussed the current development needs and the conflicts that can arise in meeting the goal of life cycle cost reduction. Whether the application is on land, at sea or in the air, the life cycle cost has a direct impact on the profitability of the power plant's operation. "To look at turbo engines only from the perspective of lower energy consumption or higher reliability would mean to stop short of what can be achieved. It is only when we appreciate the whole product life cycle, the hardware and related services that our task as engineers is given full justice. Optimizing even the piece part level maintenance, understanding the actual state of the hardware by intelligent health monitoring, and selecting the right means to optimize overhaul cycles are tasks which apply to all types of turbo engines – no matter if in the air, at sea, or on land. The difference lies less in the particular type of turbine we look at, but more in the attitude and business concept for running it. Outstanding mechanical engineering is just the beginning, the entry ticket to compete. Meeting current customer requirements is the basis; always thinking into the future makes the difference, for the city of Düsseldorf as well as for the industry."

> "To look at turbo engines only from the perspective of lower energy consumption or higher reliability would mean to stop short of what can be achieved..." Karsten Mühlenfeld, Rolls-Royce

Over 3,000 turbomachinery professionals from over 50 countries attended ASME Turbo Expo 2014

...Continued on page 83

AWARDS


R. Tom Sawyer Award


Gas Turbine Award


Aircraft Engine Technology Award


Early Career Award


Industrial Gas Turbine Technology Award


John P. Davis Award


ASME IGTI Board Chair & ASME President

Application Of An Industrial Sensor Coating System On A Rolls-Royce Jet Engine For Temperature Detection

J.P. Feist, P.Y. Sollazzo, S. Berthier, B. Charnley, J. Wells

INTRODUCTION

Engineers have continuously sought to increase fuel efficiency in gas turbines, more than halving fuel consumption over the last 3-4 decades. This was achieved mainly by increasing firing temperatures. Apart from new alloys and cooling methods, thermal barrier coatings (TBC) have played a major role in this development. These coatings were first used on jet engines in the 70's and are now a common feature on power generation turbines. TBCs allow components to survive higher temperatures and have acceptable service times. TBC technology will continue to play a dominant role in future energy solutions. TBCs are refractory coatings, usually based on yttria stabilized zirconia (YSZ), that are used to provide thermal insulation and indirectly provide oxidation protection on turbine blades, vanes and combustion chamber liners in gas turbines used in power generation and aviation. They offer the potential to allow end-users to operate at substantially higher temperatures than uncoated components could withstand. This leads directly to an increase in efficiency and a consequent reduction in CO_2 emission. The life expectancy of a TBC is known to be inversely proportional to the absolute temperature experienced by the coating. Close control of component temperatures cannot currently be achieved due to the absence of any reliable means to measure in the hot section of the engine. As a result, TBCs have, to date, been used conservatively, to extend the life of turbine components rather than to realise the full potential increase in operating temperature. Over the past 9 years Southside Thermal Sciences (STS) has pioneered the method of implementing luminescence materials into TBCs [2,5-7]. This novel approach promises optical, accurate, in-situ temperature detection and health monitoring. The basic concept is to take phosphorescent materials, as used in TV screens and energy efficient light bulbs, and embed those into standard TBC materials such as zirconia, consequently creating a 'smart' material. When illuminated with UV light this class of material starts to phosphoresce ('glow') and the observation of this light with specifically tailored instrumentation gives the engineer valuable information on temperature and structural damage such as erosion, corrosion and ageing effects as the phosphor particles act as embedded atomic sensors inside the ceramic. This paper will describe the implementation of a sensor coating system for the first time on an operating turbine providing temperature data from modified TBCs in the hot section of an operating engine.

REVIEW

The use of phosphorescent materials as temperature indicators is well known and this is an established laboratory technique and is well documented. The following references give good reviews about what is generally known as the thermographic phosphor technique [8,9]. However, the embedding of the optically active ions – namely Lanthanides and transition metals – into functional ceramics such as TBCs or even the mixing of a secondary phosphor phase into a primary material phase is a rather new concept and requires a different approach. The main consideration here is the integrity of the primary phase or primary host or the material system as such. Early failure due to the additional dopant being added is not an option as it would compromise the primary function. In the case of a TBC this is the protection of the component for many thousands of hours (e.g. 24,000 operating hours!). Choy, Feist and Heyes [1] introduced the notion of a "thermal barrier sensor coating" (sensor TBC) for temperature detection in 1998. This technique enabled surface temperature measurements, but also could provide a means to measure temperature within the TBC and at the metal/topcoat interface, hence enabling the manufacturing of an integrated heat flux gauge. The relatively low dopant levels insured no adverse effects on the coating stability. First results were published on YSZ co-doped with europium (I) powders in 2000 [10] and subsurface temperatures were measured for the first time looking through a 50µm undoped YSZ layer from a thin (≈10 µm) YSZ:Eu layer underneath [11].
Publications on industrial relevant robust coatings produced by standard production techniques appeared shortly after. The first electron beam physical vapour deposition (EBPVD) sensor coating was reported in 2001 [12] using YSZ:Dy applied with an industrial coater at Cranfield University. A more important coating technology for power generation engines, however, is the atmospheric plasma spray process (APS). First work on industrial air plasma sprayed sensor coating systems commenced around 2002 and were first published in 2005 [5,13] and later in 2006 [14]. Heyes et al. demonstrated the capabilities of APS sensor coatings for in-situ two-dimensional temperature measurements in burner rigs using a high speed camera system [13]. Further, high temperature measurement capabilities in APS coatings up to 1674K with a two material phase architecture were published by Feist et al. [14] using an industrial thermal spray coater at the Research Centre Jülich, Germany.

EXPERIMENTAL ASPECTS

TBCs are used on combustion components, the hotter rotating blades and fixed vanes in the hot gas path section of industrial gas turbines. The thermal barrier coatings on these turbines usually consist of an oxidation resistant bond coat and a ceramic insulating layer. The bond coat is normally an MCrAlY (M for metal) coating and the top coat is normally YSZ. The main function of the MCrAlY coating is to form a stable passive alumina (Al_2O_3) layer which prevents oxidation of the main components. The primary function of the YSZ layer is to prevent heat flow into the part giving a lower metal temperature thus enabling the firing temperature of the turbine to be raised without significantly degrading the mechanical properties of the base alloy of the components.

...Continued on page 78

AS THE Turbine TURNS

Gems of Turbine Efficiency

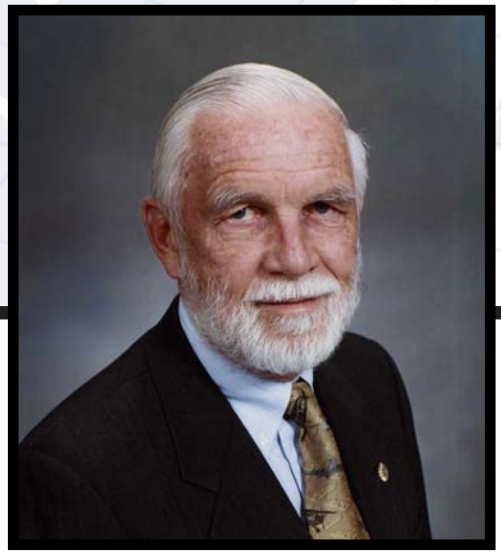

by Lee S. Langston, *Professor Emeritus, Mechanical Engineering, University of Connecticut*

This year marks the diamond jubilee for the gas turbine. Seventy five years ago, in 1939, the first jet engine aircraft flew, and the first gas turbine powering an electric generator was successfully tested.

This is also the approximate golden jubilee for the invention of turbine single crystal blades for use in gas turbines. These gas turbine "Crown Jewels" [1] were being developed and perfected at Pratt & Whitney Aircraft, when I joined the company, fresh out of graduate school, in 1964. Their first real engine test was in 1967-68 on Pratt's J58 engine, which powered the SR-71, Lockheed's supersonic reconnaissance aircraft. At that time, single crystal technology wasn't yet ready for this early application. Later, single crystal (SX) turbine blades were first used in military engines on Pratt's F100 engine, which powered the F16 and F15 fighter aircraft. Their first commercial use was on P&WA's JT9D-7R4 engine, which received FAA certification in 1982, powering Boeing's 767 and the Airbus A310 [2].

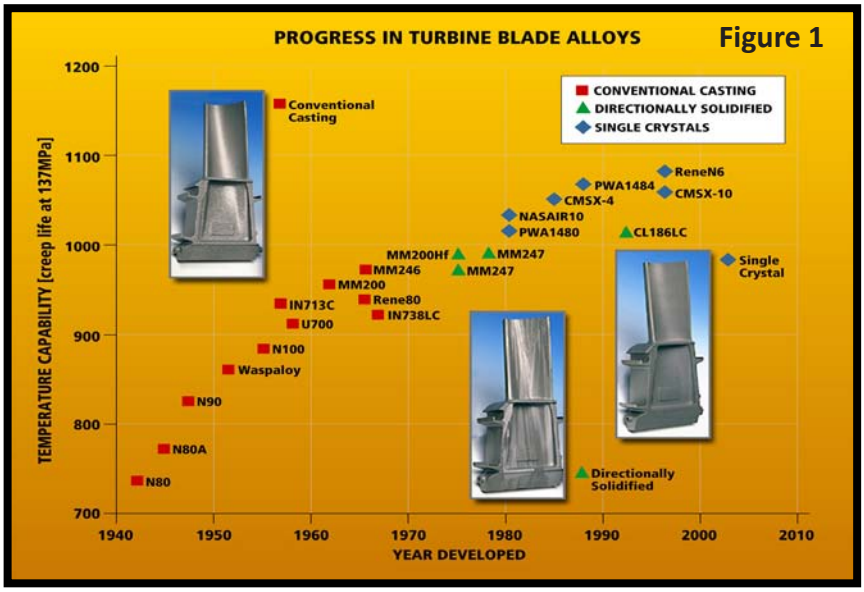

Figure 1: Progress in temperature (Celsius) creep rupture limits for various superalloys (Photos are of non-aviation turbine blades. Courtesy of NASA.)

Since these first applications, SX turbine blades have become standard on many high performance jet engines. They are also being used more recently on high performance non-aviation gas turbines, generating electric power with SX turbine blades in sizes as much as ten times larger than their aviation counterparts. (My research shows that Siemens was the first to use non-aviation SX turbine blades in their .3A series machines in the early 1990s.)

As we know, gas turbine thermal efficiency increases with greater temperatures of the gas flow exiting the combustor and entering the work-producing component —the turbine. Turbine inlet temperatures in the gas path of modern high-performance jet engines can exceed 3,000 °F, while non aviation gas turbines operate at 2,700 °F or lower. In high-temperature regions of the turbine, special high-melting-point nickel-base superalloy blades and vanes are used, which retain strength and resist hot corrosion at extreme temperatures. These superalloys, when conventionally vacuum cast, soften and melt at temperatures between 2,200 and 2,500 °F. This means blades and vanes closest to the combustor may be operating in gas path temperatures far exceeding their melting point and must be cooled to acceptable service temperatures (typically eight-to-nine-tenths of the melting temperature) to maintain integrity.

Thus, turbine airfoils subjected to the hottest gas flows take the form of elaborate superalloy investment castings to accommodate the intricate internal passages and surface hole patterns necessary to channel and direct cooling air (bled from the compressor) within and over exterior surfaces of the superalloy airfoil structure. To eliminate the deleterious effects

...Continued on next page

of impurities, investment casting is carried out in vacuum chambers. After casting, the working surface of high-temperature cooled turbine airfoils are coated with ceramic thermal barrier coatings to increase life and act as a thermal insulator (allowing inlet temperatures 100 to 300 Fahrenheit degrees higher).

Grain Boundary Phenomena

Conventionally cast turbine airfoils are polycrystalline, consisting of a three-dimensional mosaic of small metallic equiaxed crystals, or "grains", formed during solidification in the casting mold. Each equiaxed grain has a different orientation of its crystal lattice from its neighbors'. Resulting crystal lattice misalignments form interfaces called grain boundaries.

Untoward events happen at grain boundaries, such as intergranular cavitation, void formation, increased chemical activity, and slippage under stress loading. These conditions can lead to creep, shorten cyclic strain life, and decrease overall ductility. Corrosion and cracks also start at grain boundaries. In short, physical activities initiated at superalloy grain boundaries greatly shorten turbine vane and blade life, and lead to lowered turbine temperatures with a concurrent decrease in engine performance.

One can try to gain sufficient understanding of grain boundary phenomena so as to control them. But in the early 1960s, researchers at Pratt & Whitney Aircraft (now Pratt & Whitney, owned by United Technologies Corp.) set out to deal with the problem by eliminating grain boundaries from turbine airfoils altogether, by inventing techniques to cast single-crystal turbine blades and vanes.

The Result

In jet engine use, single-crystal turbine airfoils have proven to have as much as nine times more relative life in terms of creep strength and thermal fatigue resistance and over three times more relative life for corrosion resistance, when compared to equiaxed crystal counterparts. Modern high turbine inlet temperature jet engines with long life (that is, on the order of 25,000 hours of operation between overhauls) would not be possible without the use of single-crystal turbine airfoils. By eliminating grain boundaries, single-crystal airfoils have longer thermal and fatigue life, are more corrosion resistant, can be cast with thinner walls — meaning less material and less weight — and have a higher melting point temperature. These improvements all contribute to higher gas turbine thermal efficiencies.

Figure 1 shows creep life progress in turbine blade alloys, as given by NASA [3]. In the plot, the abscissa shows the year of alloy development and the ordinate shows temperature capability in degrees Celsius, for a variety of turbine blade superalloys. The temperature capability is the temperature for creep life posed as the time (1000 hours) the alloy reaches a certain elongation/strain (1%) under a given stress (137MPa = 20,000 psi). As shown, single crystal blades are clearly superior.

* * * * * * *

About fifty years ago, a small group of gas turbine industry researchers set out to eliminate grain boundaries in superalloy turbine blades. Today, the result is a whole class of single crystal turbine blades that have increased thermal efficiencies and have unmatched resistance to high-temperature creep and fatigue.

References

1. Langston, Lee S., 2006, "Crown Jewels", *Mechanical Engineering Magazine*, February, pp. 31-33.

2. Gell, M., Duhl, D.N., and Giamei, A.F., 1980, "The Development of Single Crystal Superalloy Turbine Blades", *Superalloys 1980,*

...Technical Article continued from page 75

Element	Co	Ni	Cr	Al	Y
Amdry995	38.5	2.0	21.0	8.0	0.5

Table 1: Nominal composition of the Amdry 995 MCrAlY coating

When using the after-market for coatings, the choice is more limited as only MCrAlY coating compositions not controlled by patents can be used. One of the most common is the composition known as Amdry 995. The same composition can be obtained from other powder suppliers under different names. The composition of Amdry 995 is given in Table 1. Such a coating would be a suitable coating to be used with a metal temperature of 1073-1123K. To provide suitable life for a 24,000 hours of service interval (3 years) on an industrial gas turbine it would be applied with a thickness of 250µm. The APS TBC can have a thickness from 200-1000µm depending on the component, with combustion components tending to have thicker TBCs than blades and vanes. TBC's thicker than 750µm are more prone to early failures unless pore sizes are carefully controlled. On blades and vanes for industrial gas turbines the TBC is normally 250µm.

The finished coating chosen was an Amdry 995 MCrAlY coating 250µm thick covered with an APS TBC, also 250µm thick. A back scattered scanning electron microscope image of such a coating is shown in fig. 1.

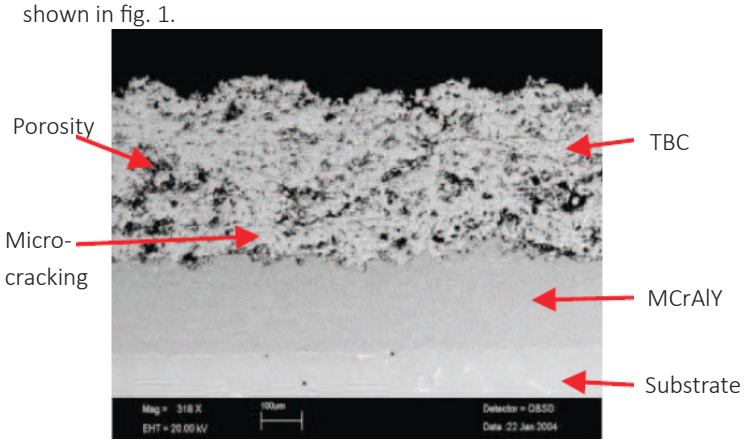

Figure 1: Example of an MCrAlY + APS TBC coating system on a large indistrial gas turbine component

With large industrial gas turbine components, adding a 250µm thick MCrAlY coating and a 250µm coating does not significantly alter the dimensions, the weight or the natural frequency of the component. On an aero-engine component such a coating could make a major difference to all of these affecting turbine performance and potentially risking a component failure. To minimise these sort of risks a much thinner coating was specified for the Viper engine. The MCrAlY was specified as being Amdry 995 or an equivalent, and the nominal MCrAlY thickness was set as 100µm. The TBC was specified as being SN_2O_4NS or an equivalent standard TBC material with modified sensor TBC powders being supplied by STS, and the nominal TBC thickness was set to between 50µm and 100µm, depending on application. The method for depositing the MCrAlY was specified as high velocity oxygen fuel for the blades and vanes, and APS for the combustor. All TBC variations were specified as being prepared by APS. The array of TBC variations trialled is shown in Table 2. Heat treatments on the parts were carried out after application of the MCrAlY. The blades were given the standard heat treatment for Nimonic 105. A spark analysis of the vanes showed the composition to be quite different from Nimonic 105 and Cranfield University identified the vanes as being manufactured from alloy G39. No standard heat treatment was available for this, and so a heat treatment typical of this type of alloy was used. The solution heat treatment was carried out at 1448K for two hours followed by ageing heat treatments of 4hrs at 1373K and 16 hours at 1023K to diffuse the coating and optimise the microstructure for operation. Even though there was a difference in deposition efficiency between the modified sensor powders and off the shelf commercial YSZ powders, all powders were found to feed well through the APS gun.

Component	Number	TBC Variation
Vane	2	Dual layer system (standard *YSZ* on the bottom 50µm thickness; STS mix on the top)
Vane	2	Dual layer system (undoped *YSZ* at bottom 50µm - 75µm thickness; doped *YSZ* on top thickness 50µm -75µm).
Vane	2	Single layer (*YSZ* doped 100µm)
Vane	2	Single layer (STS specs; 60µm) no heat treatment
Vane	2	Single layer (STS specs; 60µm) inclusive heat treatment
Blade	2	Dual layer system (standard *YSZ* on the bottom 50µm thickness; *YSZ-YAG* mix on the top)
Blade	2	EBPVD multi layer – not covered in this article
Blade	2	Single sensor layer (*YSZ* doped 100µm)
Blade	2	Single layer (STS specs; 60µm)
Blade	2	Single layer (STS specs; 60µm) inclusive heat treatment
Combustor	strips	Dual layer system (standard *YSZ* on the bottom 50µm thickness; STS mix on the top) inclusive heat treatment
Combustor	strips	Single sensor layer (*YSZ* doped 100µm)

Table 2: Array of TBC variations specified for the coating trials.

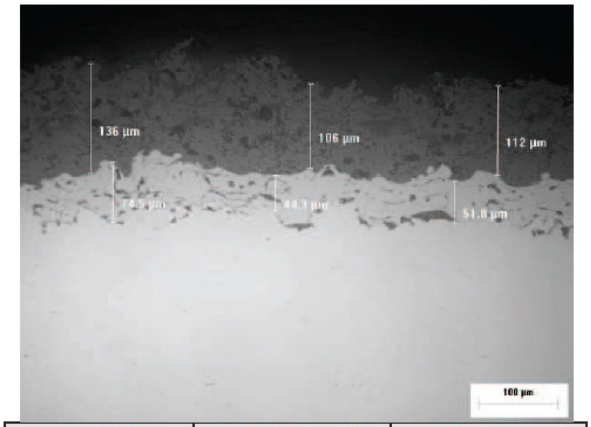

Coating layer	Specified Thickness (µm)	Actual Thickness (µm)
Key coat / bondcoat	25-50	40-70
Standard *YSZ*	50-75	50-70
STS Mix	50-75	40-60

Figure 2: Optical microscope image showing the microstructure of the top 3 layers of coating achieved for the STS Mix coating for the blade qualification (from the manufacturer coating qualification report).

One example of an APS bondcoat and APS TBC is shown in fig. 2. Parallel tests at Didcot power station revealed survivability of specific coatings in excess of 4,500 EOH. It is expected that the capability of these coatings is in the range of normal maintenance schedules of industrial gas turbines of 24,000hrs or even longer. Based on what the manufacturer learned about the powders and deposition rates during the development and production work, the manufacturer expects that with a small amount of additional development work it would be possible to improve on the current spray process.

INSTRUMENTATION AND DATA COLLECTION

The optical instrumentation for a phosphorescent thermometry system consists of the excitation optics delivering the light of a Nd:YAG laser and the collection optic. The objective was to maximize delivery power while maintaining a large distance to the actual target. This is a significant design decision as the actual optical probe can be operated outside the extreme hot section to avoid extra cooling requirements and avoid the risk of failing parts potentially jeopardizing the engine integrity.

In order to maximise the delivery energy it was decided to operate with open beam optics instead of using fibre guides. The coupling of high energy pulsed UV lasers into silica fibres is limited to relatively low power compared to an open beam. A further benefit of avoiding fibres is the absence of additional optics which would be required to refocus the light when the light exits at the fibre end. This is undesirable as the optic would decrease the delivery power on one hand and on the other hand requires additional housing making it more complex to install the probe on an engine and hence less cost-effective. The aim for the collection optic design was to achieve a large field of view with an uncooled housing. The solution came in the form of a non-imaging optic designed by STS called optical energy transfer system (OPETS) and illustrated in fig.3. The delivery of the excitation light was achieved through a beam splitter housed in a cube which is robustly attached to the front of the collection optic, hence forming a single unit. The collected phosphorescence is coupled into a 2m fibre bundle delivering the light to the remote photomultiplier tube (PMT). The collection optic also may be equipped with several wavelength selecting filters to tailor it to the observation requirements. The system maximizes light collection regardless of the distance of the source. No refocusing is needed for different distances and hence enables the operator to measure the signal without the need to adjust the optics for the right stand-off distance which would be required for a conventional optic. This is a significant advantage as it reduces the need for precise alignment in an environment where precise alignment is difficult or impossible to achieve. Another most important design feature is the large 'flat hat' transfer function guaranteeing a uniform light collection across a large field of view (Figure 4; 8 degrees). This transfer function enables the scanning or observation of moving objects across the specified field of view with very little distortion of the intensity as would potentially occur in a conventional imaging optic. The laser pulse generates a phosphorescent spot on the component shown as position 'A' in fig. 3. In case of a fast moving component such as a turbine blade the slow decreasing phosphorescence will travel with the component across the field of view (from A to C). Hence the current probe design enables the observation of the undistorted life time decay. Figure 4 shows the variation in intensity of a constant light source when moving across the field of view (FOV) of the OPETS. Between -4 and +4 degrees the probe uniformly collects light. The graph was recorded using a specialised optical bench with a LED light source. The solid lines are created using a simple interpolation. The positions A, B and C correspond to the equivalent positions in fig. 4 symbolizing a moving phosphorescent signal.

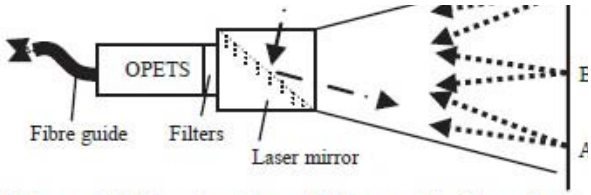

Figure 3: Illustration of the optical probe.

ROLLS-ROYCE VIPER 201 TEST BED

Two Rolls-Royce Viper Mk 201 engines were purchased by STS and a hot end instrumentation facility was designed and built at Cranfield University's Gas Turbine Engineering Laboratory. One engine was installed and commissioned as a test bed while the second engine was stripped down to remove a number of hot end components in preparation for coating by a commercial coatings company. Following the initial performance runs the first engine was dismantled, the coated components were installed and six windows were mounted on the engine enabling optical access to the main hot end components including the combustion chamber inner flame tube, nozzle guide vanes and the turbine rotor blades.

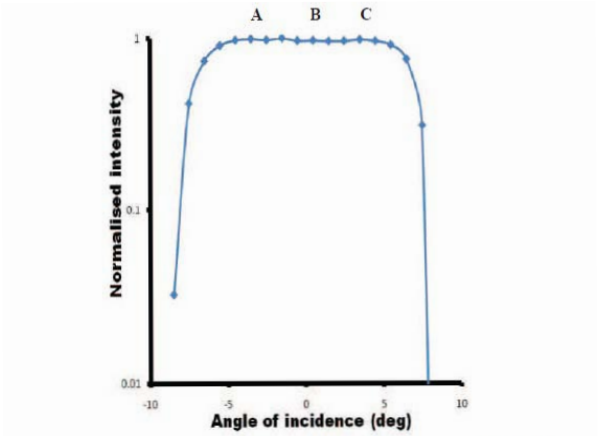

Figure 4: OPETS FOV. The positions A, B, C are equivalent to the positions in Figure 3. The flat hat function permits undistorted detection across a wide FOV.

Optical Windows

A method was required to provide clear optical access to all the hot end components; the combustion chamber, nozzle guide vanes (NGV) and turbine rotor blades. These were viewed in order of difficulty with the NGV access requiring that the window access pass through both the combustor outer casing and the outer flame tube at the correct angle onto the vane surface. The rotor window mounting plate was positioned on the downstream exhaust tube which was a more complex shape and required coordinate measuring machining and electrical discharge machining to give the necessary fit. During the design of the combustor windows it was discovered that it was possible to use dilution holes in the outer flame tube to provide sufficient FOV onto the inner flame tube surface. As it was intended to apply two different coatings to the inner flame tube, the window mounts were further adapted to extend the FOV and exploit the scanning capability of the sensor system. The extreme environment required that sapphire windows were installed and the support tubes were manufactured with a high aspect ratio to reduce issues associated with the ingress of combustion material or particles onto the optics. As the rotor windows were facing into the flow they included a purge system. Three of the six available windows are shown in fig. 5. With a view through the rotor window shown in fig. 6. The coated NGVs are shown in position in fig. 7.

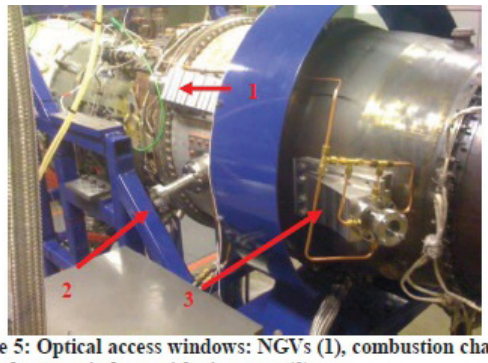

Figure 5: Optical access windows: NGVs (1), combustion chamber (2), and rotor windows with air purge (3).

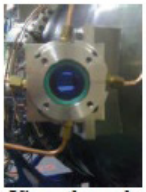

Figure 6: View through the rotor window showing the turbine blades

Figure 7: Coated NGV in position on the engine.

CALIBRATION

When a sensor TBC is excited by a short laser pulse (5ns) it starts to emit phosphoresent light. The phosphorescence decays exponentially and this decay time is usually much longer than the laser excitation pulse and is typically of the order of micro- or milliseconds. Several publications have shown the dependency between the life time decay of this phosphorescence and the temperature [5,7-11,15,16]. Figure 8 shows the phosphorescent signal at different temperatures. The life time decay is extracted by applying a single exponential fitting routine on the measured signal.

$$I(t) = I_0 e^{\left(\frac{-t}{\tau}\right)} + B_0 \qquad (1)$$

(1 is the mathematical representation of the signals illustrated in fig. 8. I_0 is the initial intensity, t is the life time decay, B_0 is the base line, and t is the time.)

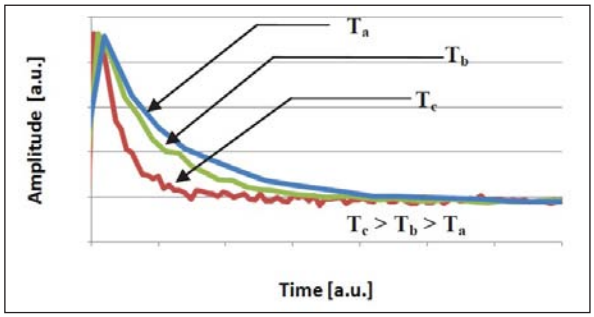

Figure 8: Phosphorescent signals at different temperatures.

In order to measure the temperature on the Viper, a correlation between the life time decay and the temperature is needed in the form of a calibration curve. The calibration curve is obtained by placing a sample inside a box furnace. The sample used for the calibration is a 30mm diameter disk coated with the same coating as the one used on the Viper components. The life time decay is measured for different temperature settings. The OPETS was placed in the front of the observation window of the furnace. Figure 9 shows a specific set-up. The Nd:YAG 355nm laser pulse is steered onto the sample by being reflected by the dichroic mirror located in the OPETS. The OPETS collected the phosphorescence signal from ca 350mm distance and the signal was guided by an optical fibre to a remote PMT. The phosphorescence signal was filtered by a band pass filter centred at 590nm. The PMT signal was amplified and digitalized. Using a computer the digitalized signal was fitted by a Levenberg-Marquardt algorithm to extract the life time decay. To automate the calibration curve measurement, the computer also controlled the furnace temperature set point. Typically the temperature of the furnace was set 20 minutes prior the measurement, providing sufficient time for the temperature to stabilise. For the Viper measurement system several calibration curves have been averaged. Each of the calibration curves were detected using slightly different settings such as: laser power, different quality phosphorescent filters, sample orientation (fig.10) and changes in the fitting routine. This was done to understand the sensitivity of the system and to estimate errors in the calibration. Figure 11 shows the resulting calibration curve which was used for the temperature detection on the Viper engine. The uncertainty associated with the

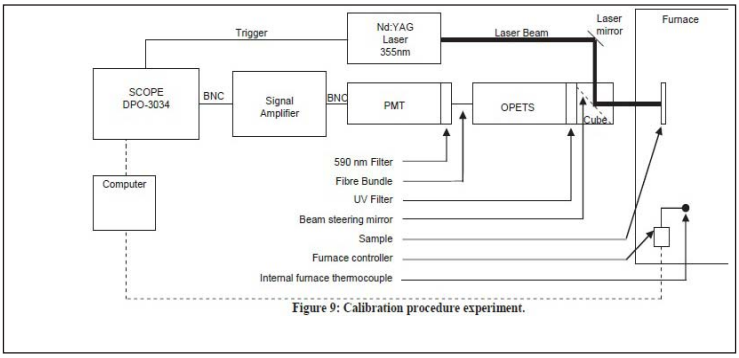

Figure 9: Calibration procedure experiment.

changed settings (laser power, filter quality, etc.) was defined as the difference between the average calibration curve and the specific curve generated for each setting. For the Viper operational regime (673K to 973K) the maximum error was determined to be ±4K, but typically was less.

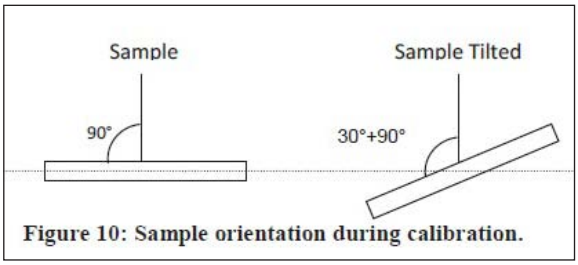

Figure 10: Sample orientation during calibration.

From fig. 11 it can be seen that the calibration curve is divided in three distinctive regimes. The first part (regime 1) from room temperature to 673K is constant and hence cannot be used for temperature detection as the life time decay does not change with temperature. The second part (regime 2), from 673K to T_Q (Q=quenching) has a low sensitivity to temperature. T_Q is defined as the temperature where the thermally activated quenching of the energy level starts to significantly dominate any other quenching process. Errors in the determination of the life time decay can result in larger errors for temperatures below T_Q as the slope is shallow (regime 2). This changes when the temperature is above T_Q as the gradient becomes very steep (range from T_Q to 1073K; regime 3). Here an error in the life time decay causes only a small error in the temperature. However, for the Viper measurements, regime 2 and 3 were both utilized.

RESULTS

The first measurement performed on the Viper was realized on a NGV as this was considered the easier task compared to the combustion chamber and the rotating blades and helped to configure the initial measurement system. Figure 12 illustrates the data collected during Run A. T_1 represents the Viper inlet temperature, T_2 the Viper compressor delivery temperature, T_3 is measured in the gas stream 40mm in front of the NGV and T_4 represents the Viper Jet pipe exhaust temperature. T_1 to T_4 were all measured using K-type thermocouples. T_s is the temperature measured on a NGV coated with the novel sensor TBC and using STS's detection technology. Data is recorded typically every second.

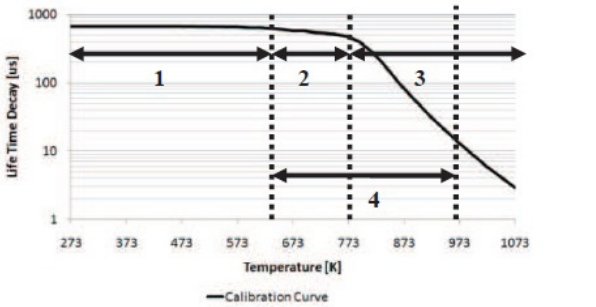

Figure 11: Calibration curve used for the *Viper* measurements using *YSZ:Dy*. (1) no temperature sensitivity, (2) low temperature sensitivity, (3) high temperature sensitivity, (4) temperature regime used for the *Viper* engine.

Most importantly T_s shows a strong correlation to the different operating conditions during the run. Under maximum load conditions at 13,500 RPM the maximum NGV temperature is detected at ca 1074K which is close to the maximum component temperature stated by the engine manual. In comparison T_3 – the gas stream temperature in the vicinity of the NGV – shows very high noise levels and it is almost impossible to detect a reliable value or follow rapid transients. The noise is probably caused by the extreme gas stream turbulences. In contrast to T_3, T_4 shows a very stable behavior throughout the test. It is significant to observe that the NGV coating temperature T_s detected by this novel sensor system correlates to the T_4 data, except for slight variations at 12k RPM. This correlation demonstrates the exceptional potential of phosphorescence sensor measurements in operating engines.

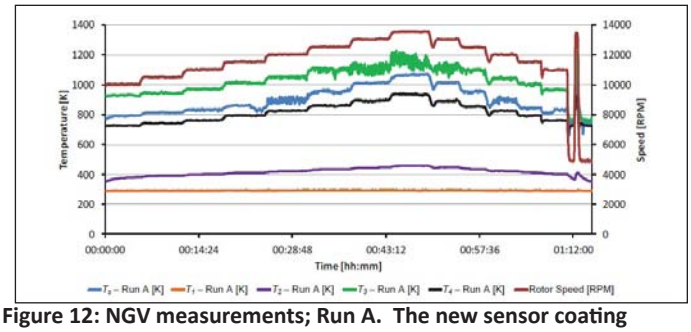

Figure 12: NGV measurements; Run A. The new sensor coating system follows the engine operating conditions well and shows very little noise.

COMBUSTION CHAMBER MEASUREMENTS

The second surface measured in the Viper was the combustion chamber inner flame tube. This measurement, Run C, was performed with the same operating conditions as shown for Run A (see fig.12) and with the same experimental setup. Optical access is provided through a window of less than 1 inch diameter. The distance between the probe and the liner surface was ca 400mm. The measurement is conducted on the inner lines therefore the signal is detected through the combustion flame. In contrast to the previous NGV

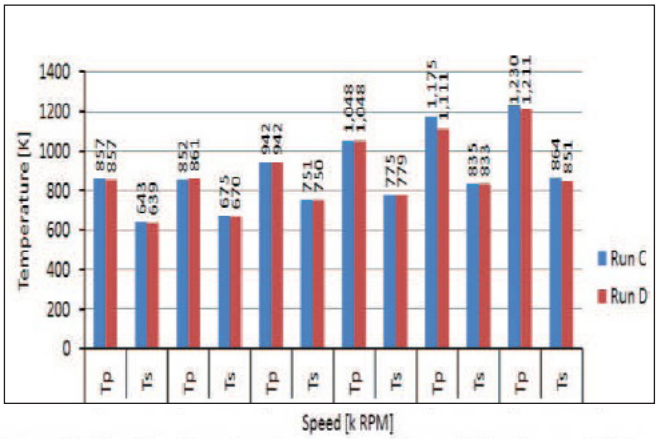

Figure 13: Combustion chamber; comparison of the Sensor TBC system with a commercial pyrometer for different speed conditions. T_p = pyrometer temperature reading; T_s = sensor coating temperature reading. The graph shows the average temperatures recorded for different operating conditions from 7,000 RPM to 13,500 RPM for two different runs. Both instruments show a remarkable repeatability.

measurements the background noise is substantially higher. This environment is very hostile for optical techniques and in particular for pyrometric measurements. As two observation windows were available for the combustion chamber, the second observation window was used to record the temperature measured by a pyrometer. This window was located directly opposite the first window looking at the equivalent position of the inner liner wall at 180°. The pyrometer was a LAND SOLOnet SN11 with a measurement range between 823K and 2023K. The pyrometer operates at a wavelength of 1mm, has a response time of 10ms and its emissivity was set to 1. Run C and D were performed using the exact same engine and instrumentation settings. The averaged temperature data for the pyrometer T_p and the sensor coating system T_s for both runs are plotted for different operating regimes indicated by different speeds in fig.13. Each operation regime lasted about 5 minutes. The commercial pyrometer T_p and the novel sensor system T_s show a high repeatability over the two runs for each operating regime. Further, in Run C and D the measured temperatures vary on average by 5K for T_s, the sensor coating system and by 15.6K for T_p, the commercial pyrometer.

At highest load the pyrometer indicates temperatures in excess of 1210K which is most unlikely as the surface of the inner liner is cooled with compressor air. The temperature of the compressor delivery air T_2 is well below 500K (see fig. 12) and hence will have a major impact on the liner temperature. An emissivity correction of the pyrometer for the ceramic surface would deliver even higher temperature readings. Further, it was observed that the gas stream temperature T_3 shows a lower temperature than T_p for the liner which is most unlikely. The authors conclude that the pyrometer data is unreliable. This is most probably due to stray light from the flame contributing to the total intensity detected by the pyrometer. Hence the pyrometer translated the extra intensity into a higher, but false, temperature reading for the liner. When comparing the T_s data recorded for the inner flame tube and for the NGV it appears that the NGV is hotter than the combustion chamber. This is not that surprising as the inner flame tube and the extreme ends of the NGV are significantly cooled using the compressor delivery air T_2.

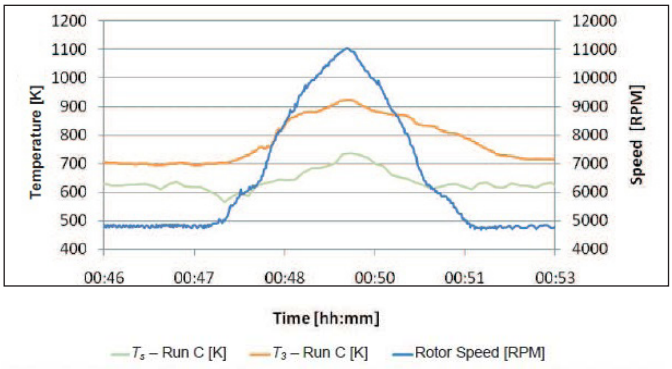

Figure 14: Rapid load increase; T_s is detected looking through a flame. The data from the inner liner can follow the strong temperature increase and shows a temperature peak at 750K.

However, the central part of the NGV where the measurements for T_s were taken is not cooled. Further the NGV takes the full load of the hot gas stream and this could explain the higher temperatures measured for T_s on the NGV in comparison to the combustion chamber.

An extra feature was introduced at the end of Run C as a rapid load increase from 5k to 11k RPM was performed (Figure 14). It can be seen that the STS system was able to follow this rapid temperature variation even when there is a high level of background noise caused by the flame. However, a noisy background above 11k RPM required an increase in integration time to ca 8 seconds for the sensor coating system. T_3 shows the gas stream temperature data is higher than the liner temperature and a difference of 190K is indicated at the peak load in fig. 14. This again is most likely an effect of the active cooling of the liner.

Turbine Blade Signal Detection

The final and most challenging task was the detection of a signal from a rotating turbine blade. The rotor disk included 113 blades of which 10 blades were coated with a sensor TBC. These ten blades consisted of five groups of two blades each. Each group received a different type of coating composition tailored for different possible operating conditions. (see Table 2). The turbine blades in the Viper engine can rotate at 13,500 RPM and this equates to ca 350m/s component velocity. The system was set to continuously fire the laser and record the resulting signal. An infrared blade detector was installed on the second optical window which enabled the tracking of individual blades – uncoated and coated. The STS system measured through the first observation window placed at 180° from the infrared blade detector. The signal from the STS measurement system could be correlated to the appropriate blade utilizing the signal from the infrared detector.

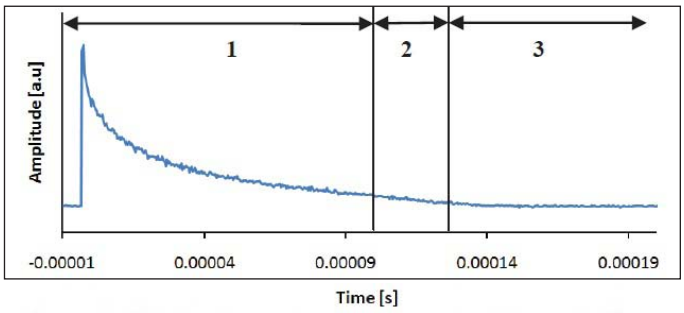

Figure 15: Life time decay phosphorescence signal from a turbine blade at a speed of 13,000 RPM using the OPETS probe. The signal from *YAG:Eu* is a single shot exposure and shows very low noise.

In order to measure the temperature on a moving part the right coating for the right temperature range and speed needs to be selected. As the temperature range in the Viper was expected to be below 1173K seven of the ten blades were equipped with 'low temperature' detection coatings. The correct sensor TBC is defined as having a phosphorescence decay lifetime short enough to be

entirely observed while the measured component passes through the field of view of the OPETS. In the current case a YAG:Eu based phosphor was used with 532nm excitation wavelength to achieve short life time decays at low temperatures. The observation wavelength was 620nm. Utilizing the OPETS an undistorted life time decay signal was observed while the object moves across the FOV. A demonstration of the signal quality is given in fig.15 at a speed of 13k RPM. The signal can be divided in three parts. The first part (marked 1 in fig.15) is the signal viewed by the OPETS when the phosphorescence spot is entirely in the FOV. The length of the observation corresponds to 50mm observation path. The observation distance is ca 400mm. In the second part (marked as 2 in fig.15) the phosphorescence spot starts to leave the FOV and this can be observed as a more rapid drop in intensity. In the last part (marked as 3 in fig.15) the phosphorescence spot was totally outside the OPETS FOV and only a base line can be observed. The temperature associated with the life time decay shown in fig. 15 was 733K. This appears too low, but corresponds very well with the 723K reading of a thermocouple buried inside the edge of a NGV which was located only 40mm upstream of the rotor and was subjected to a stream of cooling air. The validation of the data is still in progress and will be reported at a later stage.

SUMMARY AND CONCLUSION

This paper has demonstrated for the first time the feasibility of implementing an entire sensor coating system on an operating engine and successfully detecting highly precise measurements. This was only possible by pushing technical boundaries in instrumentation design and algorithm development. **Sensor coating production:** the coating is of TBC architecture and is tailored to power generation applications. It was shown that these coatings can be produced on a production line without any difficulties. The coating structure is designed to survive many thousands of hours. **Instrumentation**: an advanced optical probe was specifically designed, manufactured, characterized and implemented to enable remote detection of a moving phosphorescent spot at speeds up to 350m/s. **Precision**: the comparison of the sensor coating system with a standard thermocouple measuring the temperature in the exhaust gas stream revealed that the precision of the new system was similar to that of the thermocouple and was of the order of 5K. The calibration error was estimated to be of the same order. However, the sensor coating system detects the temperature inside the coating which is related to coating life and engine performance. The Viper engine results demonstrate the capability of such a system to provide precise temperature readings in the most difficult environment of a gas turbine. However, for temperatures reaching 1773K other types of sensor coatings would need to be adopted and have been successfully tested already [7,14].

Paper GT2012-69913, Copyright 2012 by ASME, References and Acknowledgements available by request (igtinews@asme.org).

EXHIBITION

...Continued from page 74

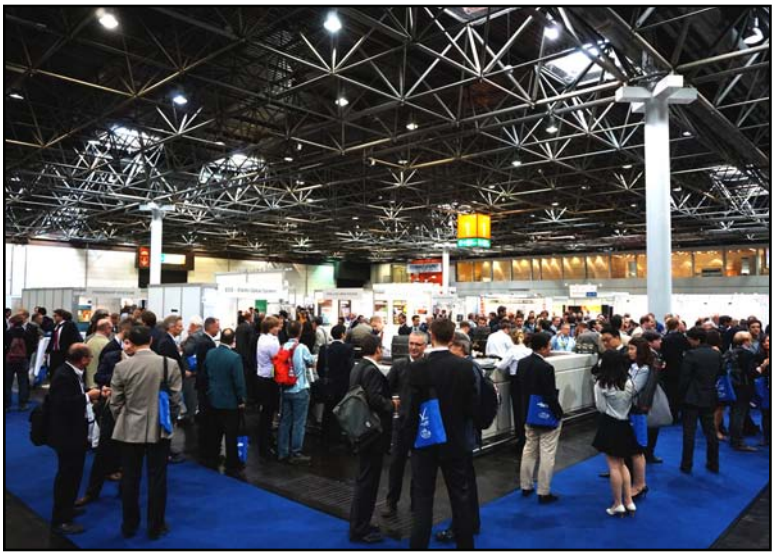

"I am attending ASME Turbo Expo 2014 because it is the place to learn new technologies, research and expand my professional career."

Turbo Expo Attendee

EXHIBIT HALL

Between sessions, attendees had the opportunity to visit the ASME Turbo Expo Exhibition Hall. From Tuesday through Thursday, the exhibit hall featured the latest technology offered by leading companies in the industry. Lunches and receptions occurred the exhibit hall each day and provided a relaxed, yet focused networking environment.

A VIEW FROM THE CHAIR

Dr. Seung Jin Song
ASME IGTI
Board Chair

Welcome back to the Global Gas Turbine News (GGTN), the quarterly news and events letter of the ASME International Gas Turbine Institute. We have had yet another record-breaking Turbo Expo in Dusseldorf with 1230 final papers (compared to 1154 papers at Turbo Expo in Copenhagen). Such sustained success is possible only with the dedication of our volunteers and staff, and I take this opportunity to thank all of you. Over the years, I have benefitted much from Turbo Expo and IGTI, and, therefore, I am particularly honored to take over the leadership of IGTI from Professor Karen Thole. She has selflessly served our community throughout her tenure on the Board, especially during the past year as the Chair. Thank you, Karen.

Recently, the IGTI Board reorganized itself to focus more on strategic issues and to develop additional leadership positions within IGTI to enable more of our members to contribute to the organization. The new five-member IGTI Board will retain focus on Turbo Expo but also look for new strategic opportunities, including regional/user-oriented IGTI events and joint efforts with other ASME groups or societies. This year's members are Piero Colonna, Howard Hodson, Allan Volponi, Vinod Philip, and myself. Reporting directly to the IGTI Board will be the newly formed Turbo Expo Executive Committee which is focused solely on organizing Turbo Expo. It will consist of the Past Chair of Conferences, Chair of Conferences, Executive Conference Chair, Technical Program Chair, Review Chair, three Vice Review Chairs, Chair of the Local Liaison Committee, and Exhibitor Representative. The Past Chair of Conferences will serve as the liaison between the IGTI Board and the Turbo Expo Executive Committee. As of now, 2015 Turbo Expo Committee members include, respectively, Howard Hodson, Geoff Sheard, Edward Hoskin, Damian Vogt, Tim Lieuwen, Jaroslaw Szwedowicz, John Chew, Anestis Kalfas, and Hany Moustapha.

Looking ahead, the Board will focus on the following :
1) Ensuring continued excellence at IGTI and Turbo Expo, starting with Turbo Expo's 60th Anniversary in 2015
2) Converting successful tracks to Committees after the recent expansion of the technical scope of IGTI (Fans & Blowers and Supercritical CO_2 tracks are planning to become Committees.)
3) Expanding globalization efforts, including more regional events (e.g. GT Latin America)
4) Strengthening support for students and early career engineers via scholarships, travel support, tutorials, and a student poster session at Turbo Expo.

For any questions regarding ASME Turbo Expo 2015, please contact Tim Graves at gravest@asme.org. If you have comments or questions, please feel free to contact me at sjsong@snu.ac.kr.

Women in Turbomachinery Event during ASME Turbo Expo this past June.
Join us in Montreal for ASME Turbo Expo 2015!